Electron-phonon quantum kinetics in pulse-excited semiconductors: Memory and renormalization effects

J. Schilp, T. Kuhn, and G. Mahler
Institut für Theoretische Physik, Universität Stuttgart, Pfaffenwaldring 57, 70550 Stuttgart, Germany
(Received 20 April 1994)

The carrier dynamics in photoexcited semiconductors is studied in a quantum-kinetic approach based on the density-matrix formalism. Besides the memory effects related to the energy-time uncertainty, we discuss interference effects between different types of interactions describing the fact that a transition due to one interaction occurs between states, which are renormalized by other interactions. We first analyze the relaxation process in a one-band model, which allows us to concentrate on memory effects in the electron-phonon interaction. We then extend the model to a two-band semiconductor interacting with a short laser pulse, which is more realistic due to the explicit treatment of the carrier generation process. Here we discuss, in particular, the role of renormalization effects. It turns out that these effects reduce the broadening due to the non-Markovian dynamics and lead to distribution functions, which are more similar to the semiclassical case; the positions of the peaks, however, exhibit slight time-dependent shifts. On the other hand, phonon quantum beats in the decay of the interband polarization are increased by these renormalization effects.

I. INTRODUCTION

On a semiclassical level the carrier dynamics in semiconductors is described by the Boltzmann equation. In this case the state of the system is completely specified in terms of the distribution functions of carriers and other quasiparticles such as, e.g., phonons. Interactions between quasiparticles lead to scattering processes between the states of the free particles. These stochastic processes are pointlike in space and time. The Boltzmann equation can be derived from quantum mechanical equations of motion after performing a series of approximations which involve, in particular, a perturbative treatment of interactions and a coarse graining in space and time.

Refinements in the experimental techniques have now led to spatial structures on a nanometer scale and to the measurement of the dynamical behavior on a femtosecond time scale. In both cases those coarse graining procedures become invalid and quantum effects related to momentum-position and energy-time uncertainty come into play. Deviations from the semiclassical behavior related to short length scales result from quantum interference phenomena leading, e.g., to resonant tunneling,[1] the Aharonov-Bohm effect,[2] or weak localization.[3] In the present work we will concentrate on quantum effects related to short time scales. We will consider a spatially homogeneous system where such quantum interference effects do not play a role.

It is now well established that for many experiments on the picosecond and the femtosecond time scale the description of the interaction of the carriers with a laser pulse cannot be expressed in terms of a generation rate. Instead, carrier-light interaction requires the introduction of a variable, the interband polarization, and the basic equations for the carrier dynamics are now given by the semiconductor Bloch equations.[4–14] The semiclassical generation rate can be recovered from the Bloch equations by performing a series of approximations. First, it is assumed that the polarization is not influenced by other types of interaction mechanisms. Under this condition the polarization can be obtained by a formal integration of its equation of motion and then can be inserted in the equations for the distribution functions. Due to this integration the generation of carriers at a given time does not depend only on the distribution of carriers at that time, but also on previous times; the generation contains memory effects. Assuming slowly varying distribution functions and light field amplitudes, a Markov approximation can be performed, resulting finally in the semiclassical generation rate.[13]

The derivation of other scattering rates, such as for carrier-phonon or carrier-carrier interactions, involves the same approximations as described above for the case of carrier-light interaction.[13] Therefore deviations from the semiclassical behavior on ultrashort time scales should be expected also for these interactions. The interaction of electrons with optical phonons is particularly well suited for an investigation of quantum kinetic phenomena since, first, it is a relatively strong interaction with typical time scales in the range of femtoseconds and, second, due to the constant energy of the phonons, deviations from the semiclassical behavior should be clearly visible.

Carrier-phonon quantum kinetics has been investigated for the case of transport in high electric fields[15–24] as well as for optically generated carriers.[25–33] The main effects related to a quantum description are a collisional broadening due to the finite lifetime of a free-carrier momentum eigenstate, collision retardation due to the description only in terms of single-particle distribution functions, and the intracollisional field effect due to the action of the electric field during the scattering process.

A major problem in treating transient phenomena on a quantum kinetic level consists in the use of the initial conditions. This is particularly true for the case of electrical transport where one is interested in early time deviations from the semiclassical model, e.g., in the velocity overshoot. Here one assumes that the coupled carrier-phonon system is in a stationary state before the application of the electric field. While in the semiclassical case the equilibrium distributions are simply given by Fermi-Dirac distributions for the carriers and Bose-Einstein distributions for phonons, as results from Boltzmann's H theorem, in the quantum case these distributions may be modified by the interactions. Therefore the initial condition should be calculated explicitly as the stationary solution of the system without field which, however, is often not easy to obtain numerically. In this respect it is advantageous for optical excitation of a semiconductor at low temperatures that there is a well-defined initial state: In an electron-hole picture this is simply given by the vacuum of electron-hole pairs. The many-particle nature of the system is contained in the material parameters, e.g., in temperature-dependent values for the gap energy and the effective masses, which are used as input parameters.

In this paper we study the quantum kinetics of optically generated carriers. Our calculations include the three kinds of quantum phenomena mentioned above: collisional broadening, collision retardation, and the intracollisional field effect. In contrast to the case of transport in static electric fields, the intracollisional field effect is related here to the field of the laser which renormalizes the system by mixing electron and hole states due to the ac Stark effect. However, not only the external field leads to this renormalization but also internal fields, e.g., due to electron-hole interaction as described in Hartree-Fock approximation, contribute to the state mixing.

The analysis of quantum kinetic phenomena can be based on several theoretical approaches. Calculations have been performed by using nonequilibrium Green's functions[22,28,34–36] leading to integro-differential equations for two-time functions, the retarded (or advanced) Green's functions, and the particle propagators. Usually, the two-time particle propagators are reduced to one-time functions, the single-particle density matrices, by a generalized Kadanoff-Baym ansatz,[35,36] which retains memory kernels in the collision terms. Alternatively, as we do in this contribution, one may start directly with the equations of motion for the single-particle density matrices.[15,25,26] This results in a hierarchy of equations of motion for different reduced density matrices which has to be truncated at some point to become accessible for a numerical investigation.

The equations of motion obtained up to a given order in perturbation theory may be different in both approaches due to the fact that perturbation theory is done with respect to a different set of variables. The second order in the density-matrix theory coincides with the result of the Green's function formalism if the equation for the particle propagator is calculated in second-order and the retarded Green's function for the noninteracting system is taken. However, as has been pointed out, this level of approximation may lead to unphysical results,[29,32] in particular the values for the distribution functions may leave the allowed interval between zero and one. In the Green's function approach this behavior is eliminated by taking into account the second-order corrections of the retarded (and advanced) functions[28,31] at least in some approximative way. In the density-matrix theory such corrections are obtained from the next level of the hierarchy by explicitly calculating two-particle correlations and inserting these quantities in the equations of motion for phonon-assisted density matrices, as will be shown in detail in Sec. II and in Appendix A.

In this paper we start with an investigation of the dynamics in a one-band semiconductor where we study the relaxation from a given initial distribution of carriers. Though not a realistic case, it allows us to concentrate on the quantum kinetic aspects of the electron-phonon interaction. At short times, due to the energy-time uncertainty, virtual transitions into states very far from the classically allowed cases are possible. Therefore, numerical results at these times may depend on the upper limit taken for the electron band. We study in particular the time dependence of the mean electron energy with respect to this upper limit.

Then we extend the model to the more realistic case of a two-band semiconductor interacting with a short laser pulse. Carrier-carrier interaction is taken into account in a screened Hartree-Fock approximation.[8] Here the time evolution starts from a well-defined initial condition, the vacuum of electron-hole pairs. We again see the time-dependent broadening due to energy-time uncertainty now for both carrier-light and carrier-phonon interactions. The most interesting difference with respect to the one-band model, however, is the fact that we now have several types of interactions. On a semiclassical level all interactions lead to transition rates which are summed up independently. In a quantum kinetic treatment the interactions interfere, describing the fact that now a transition due to one type of interaction occurs between states which are renormalized by other interactions. Incorporating these renormalizations in a self-consistent time-dependent way in a semiclassical description, even if possible in principle, would be very difficult to achieve practically because it would require a continuous change of the basis. In the quantum kinetic approach, on the other hand, this selection of the basis is not necessary. The main subject of this second part is the analysis of the role played by these interference effects. Interestingly, it turns out that some quantum features, e.g., the broadening of the distribution functions, are reduced while others, such as phonon quantum beats, are enhanced.

II. DYNAMICS IN A ONE-BAND SEMICONDUCTOR

The Hamiltonian $H = H_0 + H_{e\text{-}p}$ for a one-band semiconductor model consists of a part H_0 for describing noninteracting electrons and phonons and the electron-phonon interaction $H_{e\text{-}p}$,

$$H_0 = \sum_{\mathbf{k}} \epsilon^e_{\mathbf{k}} c^\dagger_{\mathbf{k}} c_{\mathbf{k}} + \sum_{\mathbf{q}} \hbar\omega_{\mathbf{q}} b^\dagger_{\mathbf{q}} b_{\mathbf{q}} \ , \tag{1}$$

$$H_{e\text{-}p} = \sum_{\mathbf{k},\mathbf{q}} \left[g^e_{\mathbf{q}} c^\dagger_{\mathbf{k}+\mathbf{q}} b_{\mathbf{q}} c_{\mathbf{k}} + g^{e*}_{\mathbf{q}} c^\dagger_{\mathbf{k}} b^\dagger_{\mathbf{q}} c_{\mathbf{k}+\mathbf{q}} \right] , \tag{2}$$

where $c^\dagger_{\mathbf{k}}$ ($c_{\mathbf{k}}$) and $b^\dagger_{\mathbf{q}}$ ($b_{\mathbf{q}}$) denote creation (annihilation) operators for electrons and phonons, respectively, $\epsilon^e_{\mathbf{k}} = \hbar^2 k^2/2m_e$ denotes the electron energy, m_e is the effective mass, $\hbar\omega_{\mathbf{q}}$ is the phonon energy, and $g^e_{\mathbf{q}}$ is the electron-phonon interaction matrix element. Here we will consider the case of Fröhlich interaction with LO phonons, which means a fixed phonon energy $\hbar\omega_{\mathbf{q}} = \hbar\omega_{op}$ and

$$g^e_{\mathbf{q}} = -i \left[\frac{2\pi e^2 \hbar\omega_{op}}{V} \left(\frac{1}{\varepsilon_\infty} - \frac{1}{\varepsilon_s} \right) \right]^{\frac{1}{2}} \frac{1}{q}, \tag{3}$$

with the static (ε_s) and the optical (ε_∞) dielectric constant, elementary charge e, and the normalization volume V.

The relevant observables are the distribution functions of electrons $f^e_{\mathbf{k}}$ and phonons $n_{\mathbf{q}}$,

$$f^e_{\mathbf{k}} = \langle c^\dagger_{\mathbf{k}} c_{\mathbf{k}} \rangle \quad , \qquad n_{\mathbf{q}} = \langle b^\dagger_{\mathbf{q}} b_{\mathbf{q}} \rangle \ . \tag{4}$$

The equation of motion for these distribution functions as obtained from the Heisenberg equations of motion are given by

$$\frac{d}{dt} f^e_{\mathbf{k}} = 2 \sum_{\mathbf{q}} \left[\mathrm{Re}\left\{ s^e_{\mathbf{k}+\mathbf{q},\mathbf{k}} \right\} - \mathrm{Re}\left\{ s^e_{\mathbf{k},\mathbf{k}-\mathbf{q}} \right\} \right] , \tag{5a}$$

$$\frac{d}{dt} n_{\mathbf{q}} = 2 \sum_{\mathbf{k}} \mathrm{Re}\left\{ s^e_{\mathbf{k}+\mathbf{q},\mathbf{k}} \right\} , \tag{5b}$$

where $\mathrm{Re}(x)$ denotes the real part of x. On the right-hand side in Eqs. (5) we have introduced variables, the so-called phonon-assisted density matrices s^e, which are given by the expectation values of a product of three operators weighted by the Fröhlich coupling factor $g^e_{\mathbf{q}}$,

$$s^e_{\mathbf{k}+\mathbf{q},\mathbf{k}} = \frac{i}{\hbar} g^e_{\mathbf{q}} \langle c^\dagger_{\mathbf{k}+\mathbf{q}} b_{\mathbf{q}} c_{\mathbf{k}} \rangle \ . \tag{6}$$

Equations (5) do not form a closed set of equations of motion; rather they represent the starting point of an infinite hierarchy which can only be treated approximately. The first-order contribution in carrier-phonon interaction to the dynamics of the distribution function is obtained from Eqs. (5) by factorizing the expectation value of the matrix s^e [Eq. (6)], resulting in a product of the electron distribution function $f^e_{\mathbf{k}}$ and the expectation value of a single phonon operator $\langle b_{\mathbf{q}} \rangle$. The latter one describes coherent phonons. While in inhomogeneous systems, e.g., near a surface, such contributions exist and coherent phonons have been observed experimentally,[37,38] in a homogeneous system the separation is only possible for $\mathbf{q} = 0$ and these terms cancel in Eq. (5a). Here we will restrict ourselves to the case of a homogeneous system and therefore we have to consider the next order.

To describe the dynamics of the scattering we have to determine the equation of motion of the expectation value $s^e_{\mathbf{k}+\mathbf{q},\mathbf{k}}$. It is given by

$$\begin{aligned} \frac{d}{dt} s^e_{\mathbf{k}+\mathbf{q},\mathbf{k}} = i\Omega^e_{\mathbf{k}+\mathbf{q},\mathbf{k}} s^e_{\mathbf{k}+\mathbf{q},\mathbf{k}} - \frac{1}{\hbar^2} \sum_{\mathbf{q}'} g^e_{\mathbf{q}} \big(g^e_{\mathbf{q}'} \langle c^\dagger_{\mathbf{k}+\mathbf{q}+\mathbf{q}'} c_{\mathbf{k}} b_{\mathbf{q}'} b_{\mathbf{q}} \rangle + g^{e*}_{\mathbf{q}'} \langle c^\dagger_{\mathbf{k}+\mathbf{q}-\mathbf{q}'} c_{\mathbf{k}} b^\dagger_{\mathbf{q}'} b_{\mathbf{q}} \rangle \\ - g^{e*}_{\mathbf{q}'} \langle c^\dagger_{\mathbf{k}+\mathbf{q}} c_{\mathbf{k}+\mathbf{q}'} b_{\mathbf{q}} b^\dagger_{\mathbf{q}'} \rangle - g^e_{\mathbf{q}'} \langle c^\dagger_{\mathbf{k}+\mathbf{q}} c_{\mathbf{k}-\mathbf{q}'} b_{\mathbf{q}} b_{\mathbf{q}'} \rangle \big) + \frac{1}{\hbar^2} \sum_{\mathbf{k}'} \left| g^e_{\mathbf{q}} \right|^2 \langle c^\dagger_{\mathbf{k}+\mathbf{q}} c^\dagger_{\mathbf{k}'} c_{\mathbf{k}'+\mathbf{q}} c_{\mathbf{k}} \rangle \end{aligned} \tag{7}$$

with the oscillation frequency $\Omega^e_{\mathbf{k}+\mathbf{q},\mathbf{k}} = (\epsilon^e_{\mathbf{k}+\mathbf{q}} - \epsilon^e_{\mathbf{k}} - \hbar\omega_{op})/\hbar$. On the right-hand side we have now electron-phonon and electron-electron two-particle density matrices. The second-order contribution is obtained by factorizing these two-particle density matrices into the distribution functions, e.g., according to

$$\langle c^\dagger_{\mathbf{k}+\mathbf{q}-\mathbf{q}'} c_{\mathbf{k}} b^\dagger_{\mathbf{q}'} b_{\mathbf{q}} \rangle = f^e_{\mathbf{k}} \, n_{\mathbf{q}} \, \delta_{\mathbf{q},\mathbf{q}'} \ . \tag{8}$$

This leads to an equation of motion for $s^e_{\mathbf{k}+\mathbf{q},\mathbf{k}}$ with an inhomogeneous part depending only on the distribution functions

$$\begin{aligned} \frac{d}{dt} s^e_{\mathbf{k}+\mathbf{q},\mathbf{k}} = i\Omega^e_{\mathbf{k}+\mathbf{q},\mathbf{k}} s^e_{\mathbf{k}+\mathbf{q},\mathbf{k}} + \frac{1}{\hbar^2} \left| g^e_{\mathbf{q}} \right|^2 \\ \times \Big[f^e_{\mathbf{k}+\mathbf{q}} \Big(1 - f^e_{\mathbf{k}} \Big) \Big(n_{\mathbf{q}} + 1 \Big) \\ - \Big(1 - f^e_{\mathbf{k}+\mathbf{q}} \Big) f^e_{\mathbf{k}} n_{\mathbf{q}} \Big] \end{aligned} \tag{9}$$

and thus, together with Eqs. (5), to a closed set of equations of motion.

As is well known, the semiclassical approximation is obtained by a formal solution of Eq. (9) and application of the adiabatic and Markov approximation,[13] which yields the Boltzmann equation

$$\frac{d}{dt} f^e_{\mathbf{k}} = -\Gamma^{e(\mathrm{out})}_{\mathbf{k}} f^e_{\mathbf{k}} + \Gamma^{e(\mathrm{in})}_{\mathbf{k}} \Big(1 - f^e_{\mathbf{k}} \Big) \tag{10}$$

with the rates

$$\begin{aligned} \Gamma^{e(\mathrm{in})}_{\mathbf{k}} = \frac{2\pi}{\hbar} \sum_{\mathbf{q},\pm} \left| g^e_{\mathbf{q}} \right|^2 \delta(\epsilon^e_{\mathbf{k}+\mathbf{q}} - \epsilon^e_{\mathbf{k}} \pm \hbar\omega_{op}) \\ \times f^e_{\mathbf{k}+\mathbf{q}} \Big(n_{\mathbf{q}} + \frac{1}{2} \mp \frac{1}{2} \Big) \ , \end{aligned} \tag{11a}$$

$$\Gamma_{\mathbf{k}}^{e(\mathrm{out})} = \frac{2\pi}{\hbar}\sum_{\mathbf{q},\pm}\left|g_{\mathbf{q}}^{e}\right|^{2}\delta(\epsilon_{\mathbf{k}+\mathbf{q}}^{e}-\epsilon_{\mathbf{k}}^{e}\pm\hbar\omega_{op}) \times\left(1-f_{\mathbf{k}+\mathbf{q}}^{e}\right)\left(n_{\mathbf{q}}+\frac{1}{2}\pm\frac{1}{2}\right) . \tag{11b}$$

Carrier-phonon interaction leads to scattering processes (phonon emission and absorption) between electronic states with a well-defined energy.

On a quantum kinetic level, on the other hand, the phonon-assisted density matrices are treated as independent variables. However, as already pointed out by other authors,[31,32] a solution of Eq. (9) may lead for some initial conditions to unphysical results, in particular the distribution function of electrons may become negative or larger than unity. This has also been shown analytically for the Jaynes-Cummings model, i.e., the simplified case of a two-level system with a single phonon mode.[32] Therefore, this is not a consistent level of approximation and higher-order contributions have to be taken into account. In a Green's function formalism this is done by inserting a perturbed retarded Green's function in the equation for the particle propagator.[31] In the density-matrix formalism used in this work the same result is obtained from the equations of motion of two-particle correlations, i.e., the deviations of the two-particle density matrices from their factorized form, defined, e.g., as

$$\delta\langle c_{\mathbf{k}+\mathbf{q}-\mathbf{q}'}^{\dagger}c_{\mathbf{k}}b_{\mathbf{q}'}^{\dagger}b_{\mathbf{q}}\rangle = \langle c_{\mathbf{k}+\mathbf{q}-\mathbf{q}'}^{\dagger}c_{\mathbf{k}}b_{\mathbf{q}'}^{\dagger}b_{\mathbf{q}}\rangle - f_{\mathbf{k}}^{e}n_{\mathbf{q}}\,\delta_{\mathbf{q},\mathbf{q}'} . \tag{12}$$

As shown in detail in Appendix A, the derivation of the equation of motion for each of the two-particle correlations leads to expectation values of five operators which have to be factorized into all possible combinations of single-particle and phonon-assisted density matrices. Treating the two-particle correlations in a Markov approximation and limiting ourselves to terms which have the structure of self-energy contributions, where the real part of the self-energy is neglected, the next-order contributions to Eq. (9) can be expressed in terms of a damping rate $\Gamma_{\mathbf{k}}^{e}$ related to the Boltzmann scattering rates according to

$$\Gamma_{\mathbf{k}}^{e} = \frac{1}{2}\left(\Gamma_{\mathbf{k}}^{e(\mathrm{out})}+\Gamma_{\mathbf{k}}^{e(\mathrm{in})}\right) . \tag{13}$$

Details of this derivation as well as a discussion of the approximations are given in Appendix A. The resulting equation of motion for the phonon-assisted density matrix then reads

$$\frac{d}{dt}s_{\mathbf{k}+\mathbf{q},\mathbf{k}}^{e} = \left(i\Omega_{\mathbf{k}+\mathbf{q},\mathbf{k}}^{e}-\Gamma_{\mathbf{k}+\mathbf{q}}^{e}-\Gamma_{\mathbf{k}}^{e}\right)s_{\mathbf{k}+\mathbf{q},\mathbf{k}}^{e}+\frac{1}{\hbar^{2}}\left|g_{\mathbf{q}}^{e}\right|^{2} \times\left[f_{\mathbf{k}+\mathbf{q}}^{e}\left(1-f_{\mathbf{k}}^{e}\right)\left(n_{\mathbf{q}}+1\right) -\left(1-f_{\mathbf{k}+\mathbf{q}}^{e}\right)f_{\mathbf{k}}^{e}n_{\mathbf{q}}\right] . \tag{14}$$

The set of equations of motion [Eqs. (5) and (14)] is the basis for the investigation of the quantum kinetics in a one-band model. Strictly speaking, the present formulation is still Markovian since we are dealing only with first-order differential equations. However, when compared to the semiclassical case, the set of independent variables is enlarged. Eliminating the phonon-assisted density matrices by a formal solution of Eq. (14) leads to closed integro-differential equations for the distribution functions which do contain memory kernels. Thus, when speaking of a non-Markovian dynamics in the quantum case, we refer as usual to the dynamics of the distribution functions alone.

For an isotropic initial condition $f_{\mathbf{k}}^{e}$ depends only on $k=|\mathbf{k}|$ and $s_{\mathbf{k}',\mathbf{k}}^{e}$ depends on k, k', and the angle θ between both vectors. In the case of optical phonons and a thermal phonon population, where $\omega_{\mathbf{q}}$ and $n_{\mathbf{q}}$ are independent of $\mathbf{q}$, a further simplification is possible by performing an integration over the angles and using as dynamic variables

$$F_{k}^{e} = \frac{k^{2}}{2\pi^{2}}f_{\mathbf{k}}^{e} , \tag{15a}$$

$$S_{k',k}^{e} = \frac{iV}{4\pi\hbar}\frac{k^{2}}{2\pi^{2}}\frac{k'^{2}}{2\pi^{2}} \times\iint d\phi\,d\theta\,\sin\theta\, g_{|\mathbf{k}'-\mathbf{k}|}^{e}\langle c_{\mathbf{k}'}^{\dagger}b_{\mathbf{k}'-\mathbf{k}}c_{\mathbf{k}}\rangle . \tag{15b}$$

The results described in the following have been obtained by a numerical solution of the equations of motion for these variables on a discretized mesh with constant spacing in k. Material parameters for GaAs ($m_e = 0.063$, $m_h = 0.45$, $\hbar\omega_{op} = 36.4$ meV, $\varepsilon_s = 10.92$, and $\varepsilon_\infty = 12.9$) and zero lattice temperature have been used. No hot-phonon effects are taken into account since this would require to keep the angular dependence of the phonon-assisted density matrix. Typically, 330 k values up to an electron energy of about 1 eV and a time step of 0.2 fs have been taken. The initial condition at $t=0$ is given by a distribution function which is Gaussian in energy and corresponds to that one created by a 100 fs Gaussian laser pulse (see Sec. III), as well as $S_{k',k}=0$.

In Fig. 1 we compare the relaxation dynamics of the electron energy distribution for (a) the semiclassical and (b) the quantum kinetic case. We have plotted the energy distribution, i.e., the distribution function multiplied by the density of states, as a function of energy, since this quantity gives the most intuitive picture due to the fixed separation of the phonon replicas and the conserved area under the curve. In the semiclassical case the constant phonon energy leads to the appearance of exact replicas of the initial distribution shifted downward by multiples of the phonon energy. In the quantum kinetic case each replica is initially very broad and then becomes narrower with increasing time. At early times, due to the energy-time uncertainty principle, the energy of an electron or a phonon is not yet a well-defined quantity; it needs some time to build up the energy-conserving δ function of the semiclassical transition rates. It is interesting to notice that the onset of the narrowing of

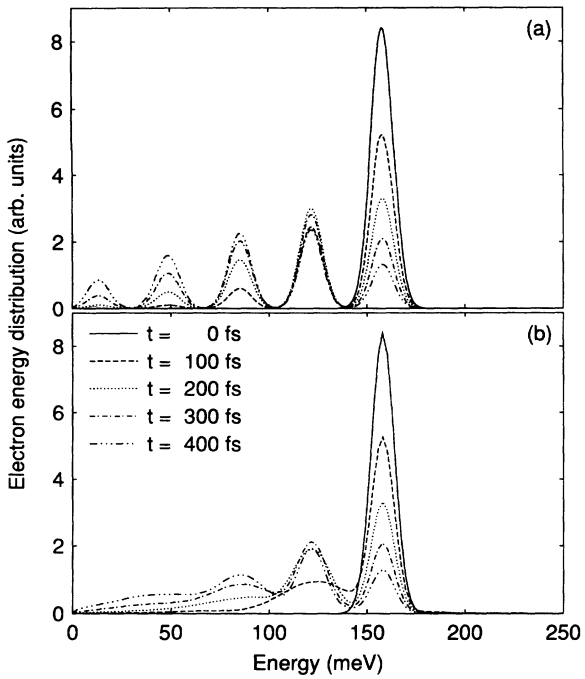

FIG. 1. The electron energy distribution $f^e(E)\sqrt{E}$ as a function of energy (a) in the semiclassical case and (b) in the quantum kinetic case at different times for relaxation from a given initial distribution in the one-band model. In (a) the relaxation leads to exact replicas of the initial distribution while in (b) the energy-time uncertainty leads to a time-dependent broadening of the replicas.

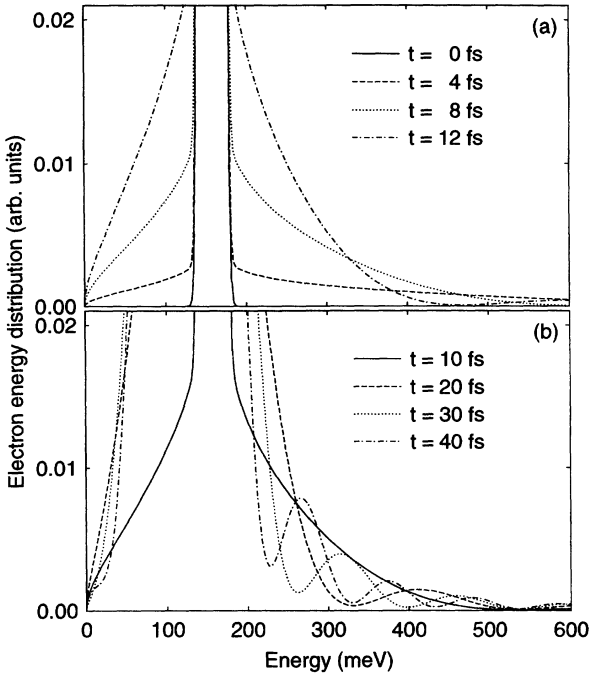

FIG. 2. The electron energy distribution $f^e(E)\sqrt{E}$ for the same case as in Fig. 1 for very short times on an enlarged scale. The curves show the buildup of the δ function according to $\sin(\omega t)/\omega$ with increasing time.

each replica shifts roughly with the phonon emission time (about 150 fs) multiplied by the number of phonons emitted. This demonstrates that an energy uncertainty is associated with each emission process. The time in the energy-time uncertainty relation is not related to the total time of the evolution starting from the initial condition at $t = 0$.

The most interesting quantum kinetic effects appear at very short times. Therefore, in Fig. 2 we show the electron energy distributions on a strongly enlarged scale. We see that indeed at early times the distribution extends up to very high energies. With increasing time the occupation of these high-energy states decreases; the decrease, however, is not a monotonous function of time, but exhibits an oscillatory behavior. Figure 2(b) shows the buildup of the energy-conserving δ function as the limit of $\sin\omega t/\omega$ as is well known from the elementary derivation of Fermi's golden rule.

In Fig. 3 the temporal evolution of the mean kinetic energy of the electrons, $\langle\epsilon\rangle = N^{-1}\sum_{\mathbf{k}} \epsilon^e_{\mathbf{k}} f^e_{\mathbf{k}}$ with $N = \sum_{\mathbf{k}} f^e_{\mathbf{k}}$, is shown. Except for the first few femtoseconds, the behavior is quite similar. The energy relaxation rate in the quantum kinetic case is slightly reduced with respect to the semiclassical case. During the first 10 fs, however, the behavior is completely different. In the semiclassical case we obtain from the Boltzmann equation (10) with a negligible phonon distribution function for the time derivative

$$\left.\frac{d}{dt}\langle\epsilon\rangle\right|^{\text{classical}} = -\frac{2\pi\omega_{op}}{N}\sum_{\mathbf{k}\mathbf{k}'}\left|g^e_{\mathbf{k}-\mathbf{k}'}\right|^2 \times\delta(\epsilon^e_{\mathbf{k}} - \epsilon^e_{\mathbf{k}'} - \hbar\omega_{op})\left(1 - f^e_{\mathbf{k}'}\right) f^e_{\mathbf{k}} , \quad (16)$$

which is always negative and, in particular, has a finite value at $t = 0$. In the quantum kinetic case at $t = 0$ the matrix S^e is zero and thus we have $d\langle\epsilon\rangle/dt = 0$. The second derivative is given by

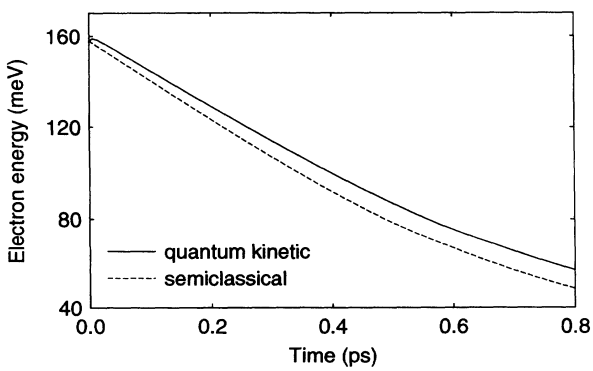

FIG. 3. Time dependence of the mean kinetic energy of the electrons for the semiclassical and the quantum kinetic case.

$$\left.\frac{d^2}{dt^2}\langle\epsilon\rangle\right|_{t=0}^{\text{quantum}} = \frac{2}{N\hbar^2}\sum_{\mathbf{k}\mathbf{k}'}\left|g^e_{\mathbf{k}-\mathbf{k}'}\right|^2 \times f^e_{\mathbf{k}}\left(1-f^e_{\mathbf{k}'}\right)\left(\epsilon^e_{\mathbf{k}'}-\epsilon^e_{\mathbf{k}}\right), \quad (17)$$

which reduces in the nondegenerate limit to

$$\left.\frac{d^2}{dt^2}\langle\epsilon\rangle\right|_{t=0}^{\text{quantum}} = \frac{2}{\hbar^2}\sum_{\mathbf{q}}\left|g^e_{\mathbf{q}}\right|^2\frac{\hbar^2q^2}{2m_e}. \quad (18)$$

The second derivative is positive and independent of the initial distribution function. It diverges if the band has no upper limit. Under the condition that initially all two-particle correlations vanish this result is exact and not limited to second order in the matrix element. Therefore, the mean energy always increases at short times. The physical reason for this fact is again the energy-time uncertainty relation: At short times all states can be occupied independent of their energy. Since there are much more states at higher energies than at lower energies, initially there are more transitions towards higher energies as can be seen from the distribution function at $t = 4$ fs in Fig. 2(a).

Figure 4 shows the time dependence of the mean electron energy at very short times for various upper limits $k_{\max}$ of the band. The number of k values has been varied in order to keep the k-step size constant. In the case of the lowest value of $k_{\max}$ the band is cut at an energy of 250 meV, i.e., about 80 meV above the initial distribution. Thus we have more states below the initial distribution than above; the energy starts with a horizontal slope and then decreases. With increasing $k_{\max}$ the number of high-energy states becomes larger and the energy exhibits an initial increase. The energy relaxation rate at later times is not affected; however, the curves remain shifted with respect to each other. These results demonstrate the problems when using a quantum kinetic model with a given initial distribution. It is related to the fact that we have started the simulation with an uncorrelated electron-phonon system, which never will build up in a real photogeneration process.

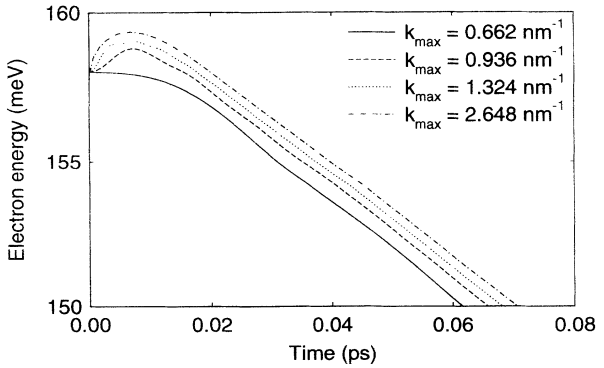

FIG. 4. Time dependence of the mean kinetic energy of the electrons for the quantum kinetic case with different values for the maximum of wave vector k corresponding to energy maxima of 0.265 eV, 0.530 eV, 1.06 eV, and 4.24 eV.

Up to now we have discussed the differences between Markovian (semiclassical) and non-Markovian (quantum kinetic) relaxation of a nonthermal carrier distribution. Due to the one-band approximation we were able to concentrate on the quantum kinetic effects related to a single type of interaction. The main drawback in this approach is related to the initial condition: The assumption that all correlations between electrons and phonons vanish at $t = 0$ would mean physically that first a distribution of electrons has to be created in the conduction band and then electron-phonon interaction is switched on. To be more realistic, the generation of the carrier distribution has to be included in the model. This can be done in the case of photoexcitation of an undoped semiconductor at low temperatures since here we start from a well-defined initial condition, the vacuum of electron-hole pairs. Such a system, a two-band semiconductor interacting with a classical light field, is the subject of the next section.

III. DYNAMICS IN A TWO-BAND SEMICONDUCTOR

We consider a two-band polar semiconductor with a direct band gap in the electron-hole picture. The full Hamiltonian

$$H = H_0 + H_{e\text{-}p} + H_{h\text{-}p} + H_L + H_{c\text{-}c} \quad (19)$$

contains the parts describing noninteracting carriers and phonons (H_0), electron-phonon ($H_{e\text{-}p}$) and hole-phonon ($H_{h\text{-}p}$) interaction, the interaction with a classical light field (H_L), and the Coulomb interaction between the carriers ($H_{c\text{-}c}$). The noninteracting part is the same as in Sec. II, extended by the holes described by creation (annihilation) operators $d^\dagger_{\mathbf{k}}$ ($d_{\mathbf{k}}$) and the hole energy $\epsilon^h_{\mathbf{k}} = E_{\text{gap}} + \hbar^2k^2/2m_h$ with the gap energy E_{gap} and the effective mass of the holes m_h. The Hamiltonians describing carrier-phonon interaction have the same structure for electrons and holes, but since the Fröhlich interaction is a polar coupling related to the electric charge, electron and hole coupling matrix elements have opposite signs $g^h_{\mathbf{q}} = -g^e_{\mathbf{q}}$. In order to trace back the various contributions in the analytical calculations, however, we will keep the different symbols for electron-phonon and hole-phonon matrix elements.

The interaction with a classical light field treated within dipole and rotating-wave approximation is given by

$$H_L = \hbar\sum_{\mathbf{k}}\left[\mu_{\mathbf{k}}c^\dagger_{\mathbf{k}}d^\dagger_{-\mathbf{k}} + \mu^*_{\mathbf{k}}d_{-\mathbf{k}}c_{\mathbf{k}}\right], \quad (20)$$

where the coupling factor

$$\hbar\mu_{\mathbf{k}} = \mathbf{M}_{\mathbf{k}}\cdot\mathbf{E}_0(t)e^{-i\omega_L t} \quad (21)$$

contains the dipole matrix element $\mathbf{M}_{\mathbf{k}}$, taken independent of $\mathbf{k}$, the central angular frequency ω_L, and the pulse shape of the electric field $\mathbf{E}_0(t)$, here taken as a

Gaussian $\mathbf{E}_0(t) = \tilde{\mathbf{E}}_0 \exp[-(t/\tau_L)^2]$. The amplitude of the field will be specified in terms of a Rabi frequency $\Omega_R = 2\mathbf{M}_\mathbf{k} \cdot \tilde{\mathbf{E}}_0/\hbar$.

In a two-band semiconductor the total carrier-carrier interaction $H_{c\text{-}c}$ via the Coulomb interaction $V_\mathbf{q}$ can be separated in three parts: electron-electron, hole-hole, and electron-hole interactions,

$$H_{c\text{-}c} = \sum_{\mathbf{k}\mathbf{k}'\mathbf{q}} V_\mathbf{q} \Big(\frac{1}{2} c^\dagger_{\mathbf{k}+\mathbf{q}} c^\dagger_{\mathbf{k}'-\mathbf{q}} c_{\mathbf{k}'} c_\mathbf{k} + \frac{1}{2} d^\dagger_{\mathbf{k}+\mathbf{q}} d^\dagger_{\mathbf{k}'-\mathbf{q}} d_{\mathbf{k}'} d_\mathbf{k} - c^\dagger_{\mathbf{k}+\mathbf{q}} d^\dagger_{\mathbf{k}'-\mathbf{q}} d_{\mathbf{k}'} c_\mathbf{k} \Big) . \quad (22)$$

We have neglected terms which do not conserve the number of particles such as Auger recombination and impact ionization, as well as the interband exchange interaction.[8] In this work we will restrict ourselves to Coulomb effects in Hartree-Fock approximation and neglect carrier-carrier scattering. Within this approximation the Hamiltonian $H_{c\text{-}c}$ can be factorized into an effective single-particle Hamiltonian $H^{\mathrm{HF}}_{c\text{-}c}$,

$$H^{\mathrm{HF}}_{c\text{-}c} = \Sigma^e_\mathbf{k} c^\dagger_\mathbf{k} c_\mathbf{k} + \Sigma^h_\mathbf{k} d^\dagger_{-\mathbf{k}} d_{-\mathbf{k}} + \Delta_\mathbf{k} c^\dagger_\mathbf{k} d^\dagger_{-\mathbf{k}} + \Delta^*_\mathbf{k} d_{-\mathbf{k}} c_\mathbf{k} \quad (23)$$

with self-energies $\Sigma^{e,h}_\mathbf{k} = -\sum_{\mathbf{q}'} V_{\mathbf{q}'} f^{e,h}_{\mathbf{k}+\mathbf{q}'}$ due to the intraband parts and an internal field $\Delta_\mathbf{k} = -\sum_{\mathbf{q}'} V_{\mathbf{q}'} p_{\mathbf{k}+\mathbf{q}'}$ due to the interband part. The self-energy part can be added to the noninteracting Hamiltonian H_0, which leads to a renormalization of the carrier energies according to $\tilde{\epsilon}^{e,h}_\mathbf{k} = \epsilon^{e,h}_\mathbf{k} + \Sigma^{e,h}_\mathbf{k}$. The internal field part can be added to the carrier-light renormalizing the external field according to $\hbar\tilde{\mu}_\mathbf{k} = \hbar\mu_\mathbf{k} + \Delta_\mathbf{k}$. Within the Hartree-Fock approximation only the coherent part of the Coulomb interaction is taken into account. The presence of free carriers leads to a screening of the bare Coulomb potential. We will not address this problem in the present work, but include the effect by using statically screened Coulomb potential in random-phase approximation with a self-consistently determined screening wave vector k_s.[39,40] The screened exchange self-energy then is supplemented by the Coulomb hole energy.[8]

In contrast to Sec. II, the Hamiltonian now contains more than one interaction mechanism. On a semiclassical level all these interactions lead to scattering processes which are simply added according to a Matthiesen rule. On a quantum mechanical level within a self-consistent calculation of the equations of motion we will see that this rule is no longer fulfilled and interference terms between different interactions appear. A main subject of this section will consist in the investigation of effects related to such cross terms in the ultrafast dynamics of photoexcited semiconductors.

The basic kinetic variables are now given by the distribution functions of electrons ($f^e_\mathbf{k}$) and holes ($f^h_{-\mathbf{k}}$) and, in order to describe the coherent coupling of the light field, the interband polarization $p_\mathbf{k} = \langle d_{-\mathbf{k}} c_\mathbf{k} \rangle$. Their equations of motion are given by

$$\frac{d}{dt} f^e_\mathbf{k} = 2\mathrm{Re}\Big\{ i\tilde{\mu}^*_\mathbf{k} p_\mathbf{k} \Big\} + 2\sum_\mathbf{q} \Big[\mathrm{Re}\Big\{ s^e_{\mathbf{k}+\mathbf{q},\mathbf{k}} \Big\} - \mathrm{Re}\Big\{ s^e_{\mathbf{k},\mathbf{k}-\mathbf{q}} \Big\} \Big] , \quad (24a)$$

$$\frac{d}{dt} f^h_{-\mathbf{k}} = 2\mathrm{Re}\Big\{ i\tilde{\mu}^*_\mathbf{k} p_\mathbf{k} \Big\} + 2\sum_\mathbf{q} \Big[\mathrm{Re}\Big\{ s^h_{-\mathbf{k}+\mathbf{q},-\mathbf{k}} \Big\} - \mathrm{Re}\Big\{ s^h_{-\mathbf{k},-\mathbf{k}-\mathbf{q}} \Big\} \Big] , \quad (24b)$$

$$\frac{d}{dt} p_\mathbf{k} = -i\Omega^p_\mathbf{k} p_\mathbf{k} - i\tilde{\mu}_\mathbf{k} \Big(1 - f^e_\mathbf{k} - f^h_{-\mathbf{k}} \Big) + \sum_\mathbf{q} \Big[t^{(+)}_{-\mathbf{k}-\mathbf{q},\mathbf{k}} - t^{(-)*}_{-\mathbf{k}+\mathbf{q},\mathbf{k}} - t^{(+)}_{-\mathbf{k},\mathbf{k}-\mathbf{q}} + t^{(-)*}_{-\mathbf{k},\mathbf{k}+\mathbf{q}} \Big] \quad (24c)$$

with $\hbar\Omega^p_\mathbf{k} = \tilde{\epsilon}^e_\mathbf{k} + \tilde{\epsilon}^h_\mathbf{k}$. These are the semiconductor Bloch equations where the relaxation part due to carrier-phonon interaction is explicitly given in terms of the intraband (s) and interband (t) phonon-assisted density matrices containing two carrier operators and one phonon operator,[32,33]

$$s^e_{\mathbf{k}+\mathbf{q},\mathbf{k}} = \frac{i}{\hbar} g^e_\mathbf{q} \langle c^\dagger_{\mathbf{k}+\mathbf{q}} b_\mathbf{q} c_\mathbf{k} \rangle , \quad (25a)$$

$$s^h_{-\mathbf{k},-\mathbf{k}-\mathbf{q}} = \frac{i}{\hbar} g^h_\mathbf{q} \langle d^\dagger_{-\mathbf{k}} b_\mathbf{q} d_{-\mathbf{k}-\mathbf{q}} \rangle , \quad (25b)$$

$$t^{(+)}_{-\mathbf{k}-\mathbf{q},\mathbf{k}} = \frac{i}{\hbar} g^e_\mathbf{q} \langle d_{-\mathbf{k}-\mathbf{q}} b_\mathbf{q} c_\mathbf{k} \rangle , \quad (25c)$$

$$t^{(-)*}_{-\mathbf{k},\mathbf{k}+\mathbf{q}} = -\frac{i}{\hbar} g^{e*}_\mathbf{q} \langle d_{-\mathbf{k}} b^\dagger_\mathbf{q} c_{\mathbf{k}+\mathbf{q}} \rangle . \quad (25d)$$

To determine the dynamics of the phonon-assisted density matrices we apply the same technique and the same approximations as discussed in Sec. II. For the matrix s^e this leads to the equation

$$\frac{d}{dt} s^e_{\mathbf{k}+\mathbf{q},\mathbf{k}} = \Big(i\Omega^e_{\mathbf{k}+\mathbf{q},\mathbf{k}} - \Gamma^e_{\mathbf{k}+\mathbf{q}} - \Gamma^e_\mathbf{k} \Big) s^e_{\mathbf{k}+\mathbf{q},\mathbf{k}} - \Big(i\tilde{\mu}_{\mathbf{k}+\mathbf{q}} + \gamma^h_{-\mathbf{k}-\mathbf{q}} \Big)^* t^{(+)}_{-\mathbf{k}-\mathbf{q},\mathbf{k}} - \Big(i\tilde{\mu}_\mathbf{k} + \gamma^h_{-\mathbf{k}} \Big) \times t^{(-)}_{-\mathbf{k},\mathbf{k}+\mathbf{q}} + \frac{\big| g^e_\mathbf{q} \big|^2}{\hbar^2} \Big[\Big(n_\mathbf{q} + 1 \Big) \Big(1 - f^e_\mathbf{k} \Big) f^e_{\mathbf{k}+\mathbf{q}} - n_\mathbf{q} f^e_\mathbf{k} \Big(1 - f^e_{\mathbf{k}+\mathbf{q}} \Big) \Big] - \frac{g^e_\mathbf{q} g^{h*}_\mathbf{q}}{\hbar^2} p^*_{\mathbf{k}+\mathbf{q}} p_\mathbf{k} . \quad (26)$$

The remaining equations for the other three types of

phonon-assisted density matrices are given in the Appendix B. Here the higher-order corrections lead, in addition to the damping rates $\Gamma_{\mathbf{k}}$, to the appearance of carrier-phonon internal fields $\gamma_{\mathbf{k}}^{e,h}$ which, neglecting again the contributions related to the principal value, are given by

$$\gamma_{\mathbf{k}}^{e,h} = \frac{\pi}{\hbar}\sum_{\mathbf{q}'} g_{\mathbf{q}'}^{e} g_{\mathbf{q}'}^{h*} \times\left[p_{\mathbf{k}-\mathbf{q}'}^{*}\,\delta(\hbar\Omega_{\mathbf{k}-\mathbf{q}',\mathbf{k}}^{e,h}) - p_{\mathbf{k}+\mathbf{q}'}\,\delta(\hbar\Omega_{\mathbf{k},\mathbf{k}+\mathbf{q}'}^{e,h})\right] \tag{27}$$

(see Appendix B).

Let us now discuss the different contributions entering on the right-hand side of Eq. (26). The terms involving s^e and the square brackets agree with the one-band model discussed in Sec. II. As we have seen there, after performing a Markov approximation these terms give rise to the usual Boltzmann scattering rates for electron-phonon interaction where the damping leads to collisional broadening. They involve only the electron-phonon matrix element $g_{\mathbf{q}}^{e}$. The last term contains electron-phonon and hole-phonon interaction simultaneously. It is related to the presence of a definite phase relation between electrons and holes characterized by the interband polarization and is sometimes called polarization scattering.[11]

The most interesting terms are those which couple different types of phonon-assisted density matrices. This coupling is due to three different mechanisms: carrier-light interaction ($\mu_{\mathbf{k}}$), electron-hole interaction ($\Delta_{\mathbf{k}}$), and the simultaneous interaction of electrons and holes with phonons ($\gamma_{\mathbf{q}}^{h}$). Remembering that the definition of the matrix s already includes an electron-phonon matrix element, we see that indeed these terms describe interference effects between different types of interactions. Since they couple different phonon-assisted density matrices, there is no more a direct way to formally integrate Eq. (26) and then perform a Markov approximation to obtain the semiclassical limit. Instead, one first had to transform the matrices s and t into a new set of variables given by linear combinations of s and t which satisfy uncoupled equations of motion. This transformation would lead to shifted frequencies and thus, after a Markov limit, to different arguments in the δ functions of the scattering rates. Therefore, these terms describe the fact that the scattering does not occur between the unperturbed states of the noninteracting carriers, but rather between states which are renormalized due to the presence of other interactions. In the present case these renormalizations involve, in particular, the mixing between electron and hole states due to the light field (ac Stark effect), the electron-hole interaction (excitonic effects), and the carrier-phonon interaction (interband polaron effect). Therefore, these contributions describe an intracollisional field effect, where the field consists of the applied laser field as well as contributions due to internal fields. The mixing of states with different $\mathbf{k}$ values due to intraband polaron effects as described by the off-diagonal contributions in Eq. (A3) could also be included, but in the present calculations it has been neglected since it is expected to be of minor importance with respect to the light- and exciton-induced effects (see the discussion in Appendix A).

For practical purposes, however, such a diagonalization procedure is, in general, not tractable because these renormalizations themselves are influenced by the dynamics of the system. They are time dependent and would thus require a diagonalization procedure to be performed at each time. Therefore it is difficult to treat such effects on the semiclassical level. On the quantum kinetic level discussed here, on the other hand, they are easy to include. They hardly increase the computer time since most of the quantities have to be calculated anyway.

The numerical investigations are based on the closed set of equations of motion given by Eqs. (24), (26), and (B1) where again, as described in Sec. II, an integration over the angular variables is performed. In most cases a laser pulse with a pulse duration of $\tau_L = 100$ fs, a Rabi frequency of $\Omega_R = 5\ \mathrm{ps}^{-1}$, and an excess energy of $E_{\mathrm{exc}} = \hbar\omega_L - E_{\mathrm{gap}} = 180$ meV has been used.

First we have switched off all contributions related to the interference between different interactions describing the renormalization effects. Thus we will see only effects associated with the non-Markovian character of the quantum kinetic model. The terms quadratic in the interband polarization are included; however, it turns out that they have a negligible influence on the dynamics. In Fig. 5 the electron energy distribution is plotted at different times. The time-dependent broadening is now due to both carrier-light and carrier-phonon interactions. The former one dominates at short times [Fig. 5(a)] leading to a narrowing of the first (unrelaxed) peak in the dis-

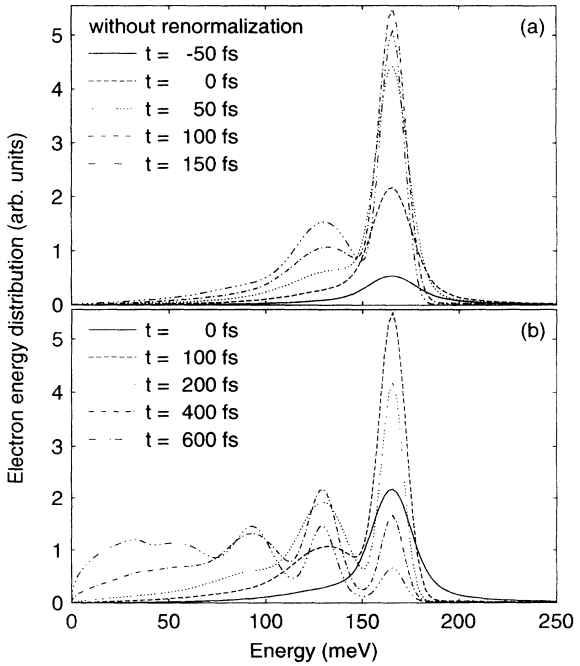

FIG. 5. The electron distribution function $f^e(E)\sqrt{E}$ as a function of energy for the two-band model excited by a 100 fs laser pulse at different times without renormalization terms between different interactions.

tribution function with increasing time. After the pulse is over, the peak has reached its final width. Carrier-phonon interaction, as in the one-band case, leads to a narrowing of each phonon replica from an initially broad underground with increasing time [Fig. 5(b)] until the semiclassical width is reached. The times when a local minimum between two subsequent replicas starts to build up, are, approximately, $t = 50$ fs, $t = 200$ fs, $t = 400$ fs, and $t = 600$ fs, respectively; thus they are again roughly separated by the semiclassical phonon emission time indicating that an energy-time uncertainty is connected with each emission process.

In Fig. 6 now the interference terms [second row in Eq. (26)] are included in the simulation. When comparing the results with the previous case (Fig. 5), two characteristic differences become obvious. First, the interference terms result in a narrowing of the phonon replicas. This can clearly be seen by looking, e.g., at the distribution functions at $t = 50$ fs or $t = 150$ fs. A minimum between the generated peak and the first replica can now be identified already at $t = 0$ fs. Thus we obtain the interesting result that including additional quantum mechanical features in the model leads to a dynamics which becomes more similar to the semiclassical behavior. The second feature is most clearly seen in Fig. 6(b). In contrast to Fig. 5, the position of the maxima of the peaks now becomes time dependent. This is a direct consequence of the renormalization due to light field and the excitonic effects. It should be noted that the energy scale of the abscissa always refers to the band structure of non-interacting electrons.

In order to see better the differences between the various approaches, we have plotted in Fig. 7 the electron

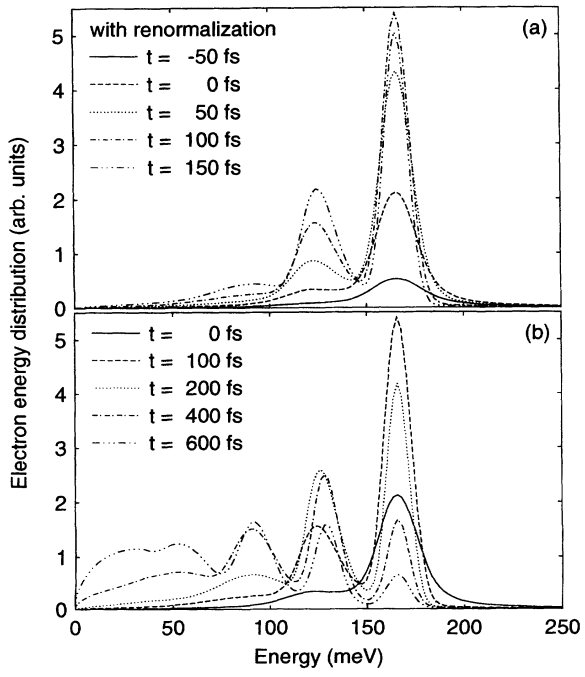

FIG. 6. Same as Fig. 5, but including the renormalization terms. These terms lead to a narrowing and to shifts of the maxima due to renormalization effects.

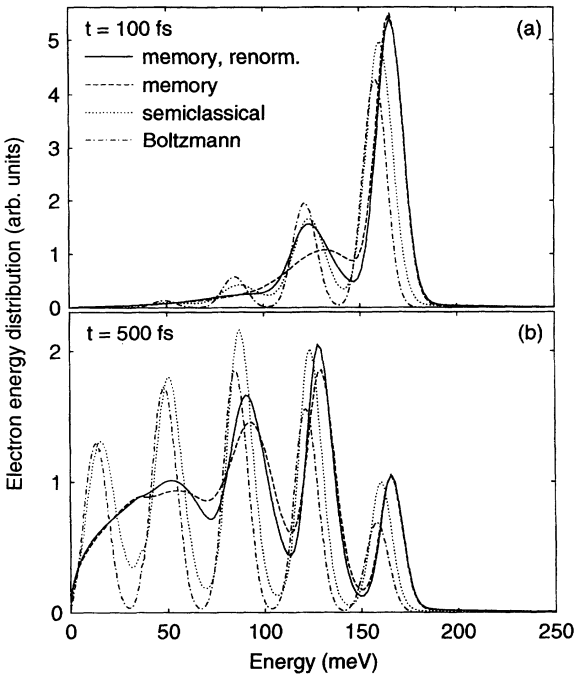

FIG. 7. The electron energy distribution $f^e(E)\sqrt{E}$ as a function of energy for the two-band model excited by a 100 fs laser pulse at two different times calculated within the quantum kinetic model with and without renormalization terms, with the Bloch equations including semiclassical phonon scattering rates, and with the Boltzmann equation including a semiclassical carrier generation rate.

energy distributions at two fixed times for the quantum kinetic model with (solid lines) and without (dashed lines) renormalization terms, the Bloch equation model with semiclassical carrier-phonon scattering rates (dotted lines), and the Boltzmann model where also the carrier generation is described by a semiclassical rate. The shift in the peak positions of the quantum kinetic and the semiclassical results are due to the polaron shift in the generation process which is automatically included when calculating the phonon-assisted density matrices, while it has been neglected in the semiclassical treatment of carrier-phonon interaction. The slight shifts between the Bloch equations with semiclassical scattering and the Boltzmann equation is due to Hartree-Fock terms which are not included in the latter equation. We again see the remarkably faster narrowing of the peaks if the renormalization terms are included in the quantum kinetic model, as well as the delay in the narrowing of subsequent replicas.

Finally, Fig. 8 shows the mean energy of electrons and holes as a function of time. In this integrated quantity we find no difference between the quantum kinetic cases with and without renormalization effects. During the pulse the main difference is related to the carrier generation process which involves an energy-time uncertainty in the solid and dotted curves while in the Boltzmann case the spectral shape of the generation rate is always given by the Fourier transform of the pulse. The energy relaxation rates are again very similar, being slightly smaller in the

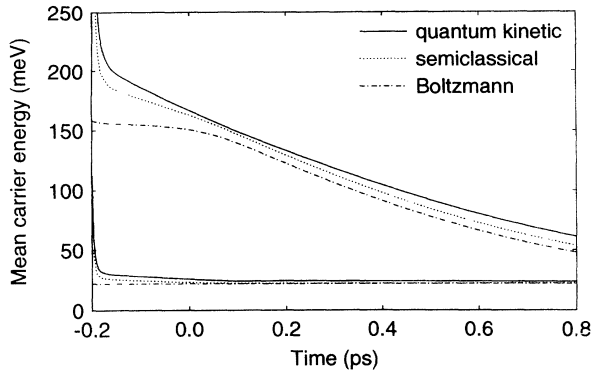

FIG. 8. Time dependence of the mean kinetic energy of electrons and holes for the various models.

quantum kinetic case.

All these quantum effects lead only to relatively small quantitative changes in the carrier dynamics and would thus be very difficult to observe experimentally. As we have seen, the situation becomes even worse with renormalization effects included because in this case the distribution functions are even closer to the semiclassical case. However, as recently pointed out,[31] in an experiment measuring the interband polarization the situation might be different. Here the quantum kinetics should lead to the appearance of phonon quantum beats which are absent in the semiclassical case. These quantum beats can be explained as a beating between the direct and the phonon-assisted transitions. It has been pointed out that under realistic conditions they are visible in the calculation only if the Hartree-Fock terms are included. Now the question arises as to whether these quantum beats are also modified by the presence of renomalization effects. To investigate this point we use the same parameters as in Ref. 31: a pulse duration of $\tau_L = 50$ fs, a Rabi frequency of $\Omega_R = 40$ ps^{-1}, and an excess energy of $E_{\mathrm{exc}} = 60$ meV.

In Fig. 9 the incoherently summed polarization $p^{\mathrm{inc}} = \sum_{\mathbf{k}} |p_{\mathbf{k}}|$ is plotted as a function of time for different cases (a) without and (b) with Hartree-Fock terms. During the pulse the Rabi oscillation is stronger including the Hartree-Fock terms due to the Coulomb enhancement described by the internal field. After the pulse the dephasing of the coherence in the system is seen for all cases; the overall dephasing rate is nearly independent of the model. Within a semiclassical description of the relaxation process the incoherently summed polarization decays monotonically and also the dashed line in Fig. 9(a) for the quantum kinetic model without Hartree-Fock and interference terms exhibits practically no structure, in agreement with Ref. 31. When comparing the solid line in Fig. 9(a) with the dashed line in Fig. 9(b), we see that Hartree-Fock terms as well as interference terms now lead to the appearance of quantum beats with approximately the same amplitude. The reason is that both renormalization and excitonic effects increase the pair coherence in the system by mixing electron and hole states. These phonon quantum beats are strongly enhanced if both effects are included [solid line in Fig. 9(b)]. Thus, in contrast to the case of the distribution functions, quantum effects are increased here by renormalization effects which might enhance the possibility of experimental observation.

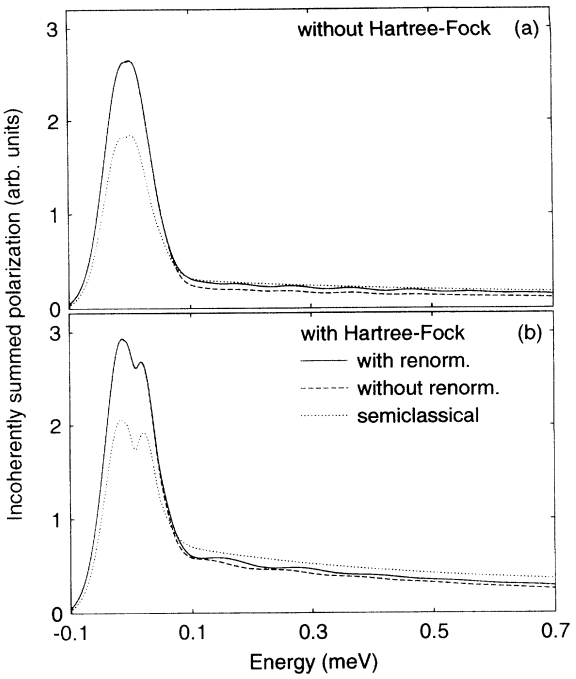

FIG. 9. Incoherently summed polarization $\sum_{\mathbf{k}} |p_{\mathbf{k}}|$ as a function of time (a) without and (b) with Hartree-Fock terms. The phonon quantum beats are most pronounced if both Hartree-Fock and renormalization terms are included.

IV. CONCLUSIONS

We have presented an analysis of the electron-phonon quantum kinetics in a one-band and a two-band semiconductor. In the case of a one-band model the relaxation of a given initial distribution has been investigated. Though not a realistic situation, it allowed us to concentrate on the quantum effects related to electron-phonon interaction. We have seen the time-dependent broadening of the phonon replicas due to energy-time uncertainty and the build up of the δ function, which describes the energy conserving in the semiclassical limit, according to a $\sin(\omega t)/\omega$ in the distribution function. While in the semiclassical case the mean electron energy at low lattice temperatures always decreases, in the quantum kinetic case it starts with a horizontal slope and then increases at short times. This increase is sensitive to the upper limit of the band in the simulation and is related to the use of an initial condition where electrons and phonons are taken to be uncorrelated. The subsequent energy relaxation is slightly reduced with respect to the semiclassical model.

We then have investigated a more realistic situation, a two-band semiconductor excited by a short laser pulse. We saw again the time-dependent broadening of the generated peak and of the replicas now due to both carrier-

light and carrier-phonon interaction. We have shown that in a quantum kinetic treatment an interference between different types of interactions, corresponding to time-dependent renormalization effects in the dynamics, can be included. They lead to slight time-dependent shifts of the positions of the peak maxima in the electron energy distribution. Surprisingly, however, it turned out that by including these quantum mechanical effects the broadening is reduced and the energy distributions therefore look more similar to the semiclassical case. On the other hand, these interband renormalization effects increase the amplitude of phonon quantum beats in the relaxation of the incoherently summed polarization due to an increase of the pair coherence.

ACKNOWLEDGMENTS

We thank H. Haug, D. B. Tran Thoai, R. Zimmermann, J. Wauer, and F. Rossi for valuable discussions.

APPENDIX A

Here we derive the higher-order corrections to the equations of motion for the phonon-assisted density matrices resulting from two-particle correlations. As an example we take the variable $\delta\langle c^\dagger_{\mathbf{k}+\mathbf{q}-\mathbf{q}'}c_{\mathbf{k}}b^\dagger_{\mathbf{q}'}b_{\mathbf{q}}\rangle$. The equation of motion for the corresponding two-particle electron-phonon density matrix is given by

$$\begin{aligned}\frac{d}{dt}\langle c^\dagger_{\mathbf{k}+\mathbf{q}-\mathbf{q}'}c_{\mathbf{k}}b^\dagger_{\mathbf{q}'}b_{\mathbf{q}}\rangle &= \frac{i}{\hbar}\left(\epsilon^e_{\mathbf{k}+\mathbf{q}-\mathbf{q}'}-\epsilon^e_{\mathbf{k}}\right)\langle c^\dagger_{\mathbf{k}+\mathbf{q}-\mathbf{q}'}c_{\mathbf{k}}b^\dagger_{\mathbf{q}'}b_{\mathbf{q}}\rangle \\ &+\frac{i}{\hbar}\sum_{\mathbf{q}''}\Big\{g^e_{\mathbf{q}''}\left[\langle c^\dagger_{\mathbf{k}+\mathbf{q}-\mathbf{q}'+\mathbf{q}''}c_{\mathbf{k}}b_{\mathbf{q}''}b^\dagger_{\mathbf{q}'}b_{\mathbf{q}}\rangle-\langle c^\dagger_{\mathbf{k}+\mathbf{q}-\mathbf{q}'}c_{\mathbf{k}-\mathbf{q}''}b_{\mathbf{q}''}b^\dagger_{\mathbf{q}'}b_{\mathbf{q}}\rangle\right] \\ &+g^{e*}_{\mathbf{q}''}\left[\langle c^\dagger_{\mathbf{k}+\mathbf{q}-\mathbf{q}'-\mathbf{q}''}c_{\mathbf{k}}b^\dagger_{\mathbf{q}''}b^\dagger_{\mathbf{q}'}b_{\mathbf{q}}\rangle-\langle c^\dagger_{\mathbf{k}+\mathbf{q}-\mathbf{q}'}c_{\mathbf{k}+\mathbf{q}''}b^\dagger_{\mathbf{q}''}b^\dagger_{\mathbf{q}'}b_{\mathbf{q}}\rangle\right]\Big\} \\ &+\frac{i}{\hbar}\sum_{\mathbf{k}''}\left\{g^e_{\mathbf{q}'}\langle c^\dagger_{\mathbf{k}+\mathbf{q}-\mathbf{q}'}c_{\mathbf{k}}c^\dagger_{\mathbf{k}''+\mathbf{q}'}c_{\mathbf{k}''}b_{\mathbf{q}}\rangle-g^{e*}_{\mathbf{q}}\langle c^\dagger_{\mathbf{k}+\mathbf{q}-\mathbf{q}'}c_{\mathbf{k}}c^\dagger_{\mathbf{k}''}c_{\mathbf{k}''+\mathbf{q}'}b^\dagger_{\mathbf{q}'}\rangle\right\}. \end{aligned} \tag{A1}$$

On the right-hand side expectation values of five operators, phonon-assisted two-particle density matrices appear. After factorization into all possible combinations of distribution functions and phonon-assisted density matrices and inserting the equations of motion of the distribution functions according to

$$\frac{d}{dt}\,\delta\langle c^\dagger_{\mathbf{k}+\mathbf{q}-\mathbf{q}'}c_{\mathbf{k}}b^\dagger_{\mathbf{q}'}b_{\mathbf{q}}\rangle = \frac{d}{dt}\langle c^\dagger_{\mathbf{k}+\mathbf{q}-\mathbf{q}'}c_{\mathbf{k}}b^\dagger_{\mathbf{q}'}b_{\mathbf{q}}\rangle - \frac{d}{dt}\left(f^e_{\mathbf{k}}n_{\mathbf{q}}\right)\delta_{\mathbf{q},\mathbf{q}'}\,, \tag{A2}$$

we obtain

$$\begin{aligned}&\frac{d}{dt}\,\delta\,\langle c^\dagger_{\mathbf{k}+\mathbf{q}-\mathbf{q}'}c_{\mathbf{k}}b^\dagger_{\mathbf{q}'}b_{\mathbf{q}}\rangle-\frac{i}{\hbar}\left(\epsilon^e_{\mathbf{k}+\mathbf{q}-\mathbf{q}'}-\epsilon^e_{\mathbf{k}}\right)\delta\,\langle c^\dagger_{\mathbf{k}+\mathbf{q}-\mathbf{q}'}c_{\mathbf{k}}b^\dagger_{\mathbf{q}'}b_{\mathbf{q}}\rangle \\ &=\frac{g^e_{\mathbf{q}'}}{g^e_{\mathbf{q}}}\left(1-f^e_{\mathbf{k}+\mathbf{q}-\mathbf{q}'}+n_{\mathbf{q}'}\right)s^e_{\mathbf{k}+\mathbf{q},\mathbf{k}}-\frac{g^e_{\mathbf{q}'}}{g^e_{\mathbf{q}}}\left(f^e_{\mathbf{k}}+n_{\mathbf{q}}\right)s^e_{\mathbf{k}+\mathbf{q}-\mathbf{q}',\mathbf{k}-\mathbf{q}'} \\ &-\frac{g^{e*}_{\mathbf{q}}}{g^{e*}_{\mathbf{q}'}}\left(f^e_{\mathbf{k}+\mathbf{q}-\mathbf{q}'}+n_{\mathbf{q}'}\right)s^{e*}_{\mathbf{k},\mathbf{k}-\mathbf{q}'}+\frac{g^{e*}_{\mathbf{q}}}{g^{e*}_{\mathbf{q}'}}\left(1-f^e_{\mathbf{k}}+n_{\mathbf{q}}\right)s^{e*}_{\mathbf{k}+\mathbf{q},\mathbf{k}+\mathbf{q}-\mathbf{q}'}\,. \end{aligned} \tag{A3}$$

We now apply the adiabatic and Markov approximation to this equation. Formally we have an equation of motion $\dot z - i\Omega z = \sum_i y_i$ for the variable z, denoting the two-particle correlation, with a frequency Ω and inhomogeneous parts y_i, which can be separated into slowly varying parts $\tilde y_i$ and rapid oscillations due to the free rotation of the phonon-assisted density matrices according to $y_i = \tilde y_i \exp(-i\omega_i t)$. The approximations lead to the semiclassical solution

$$z = \sum_i\left[\pi\,\delta(\Omega-\omega_i)+i\,\mathcal{P}\left(\frac{1}{\Omega-\omega_i}\right)\right]y_i \tag{A4}$$

with Dirac's delta function $\delta(x)$ and the principal value $\mathcal{P}(1/x)$. The imaginary part involving the principal values leads to polaron shifts in the energies and will be neglected here.

As a result we now have expressed the two-particle correlations in terms of phonon-assisted density matrices. Remembering from Eq. (7) that the contribution to the equation of motion of $s^e_{\mathbf{k}+\mathbf{q},\mathbf{k}}$ involves a summation over $\mathbf{q}'$, we see that, while in the first term on the right-hand side the summation is performed only over positive quantities, in the other three terms also the complex quantity s^e is involved in the summation. Since in gen-

eral this quantity is rapidly oscillating in time, we may neglect these terms by using a random-phase approximation. This assumption is equivalent to the calculation of the dephasing rate in a two-band model as the total scattering rate. In the language of Green's functions it means that we take only the self-energy part for the retarded Green's function.[31]

Within these approximations the two-particle correlation is given by

$$\delta\langle c^{\dagger}_{\mathbf{k}+\mathbf{q}-\mathbf{q}'} c_{\mathbf{k}} b^{\dagger}_{\mathbf{q}'} b_{\mathbf{q}}\rangle = \pi\delta(\Omega^{e}_{\mathbf{k}+\mathbf{q},\mathbf{k}+\mathbf{q}-\mathbf{q}'}) \frac{g^{e}_{\mathbf{q}'}}{g^{e}_{\mathbf{q}}} \left(1 - f^{e}_{\mathbf{k}+\mathbf{q}-\mathbf{q}'} + n_{\mathbf{q}'}\right) s^{e}_{\mathbf{k}+\mathbf{q},\mathbf{k}} \,. \tag{A5}$$

The same calculations have to be performed for the other two-particle correlations in Eq. (7). It should be noted that on this level also the two-particle density matrices involving two phonon annihilation operators, where the factorized part vanishes, give a finite contribution. As a final results we obtain an additional term in Eq. (9) due to the correlations

$$\left.\frac{d}{dt} s^{e}_{\mathbf{k}+\mathbf{q},\mathbf{k}}\right|^{\mathrm{corr}} = -\left(\Gamma^{e}_{\mathbf{k}+\mathbf{q}} + \Gamma^{e}_{\mathbf{k}}\right) s^{e}_{\mathbf{k}+\mathbf{q},\mathbf{k}} \tag{A6}$$

with the Boltzmann relaxation rates according to Eqs. (11) and (13) and thus the equation of motion (14).

APPENDIX B

For completeness the equations of motion for the remaining phonon-assisted density matrices s^{h}, $t^{(+)}$, and $t^{(-)}$ in the two-band model are given here. Their structure is the same as for s^{e} discussed in Sec. III:

$$\frac{d}{dt} s^{h}_{-\mathbf{k},-\mathbf{k}-\mathbf{q}} = \left(i\Omega^{h}_{-\mathbf{k},-\mathbf{k}-\mathbf{q}} - \Gamma^{h}_{-\mathbf{k}} - \Gamma^{h}_{-\mathbf{k}-\mathbf{q}}\right) s^{h}_{-\mathbf{k},-\mathbf{k}-\mathbf{q}} + \left(i\tilde{\mu}_{\mathbf{k}} + \gamma^{e}_{\mathbf{k}}\right)^{*} t^{(+)}_{-\mathbf{k}-\mathbf{q},\mathbf{k}} + \left(i\tilde{\mu}_{\mathbf{k}+\mathbf{q}} + \gamma^{e}_{\mathbf{k}+\mathbf{q}}\right) t^{(-)}_{-\mathbf{k},\mathbf{k}+\mathbf{q}}$$
$$+ \frac{1}{\hbar^2}\left|g^{h}_{\mathbf{q}}\right|^{2}\left[\left(n_{\mathbf{q}}+1\right)\left(1 - f^{h}_{-\mathbf{k}-\mathbf{q}}\right) f^{h}_{-\mathbf{k}} - n_{\mathbf{q}} f^{h}_{-\mathbf{k}-\mathbf{q}}\left(1 - f^{h}_{\mathbf{k}}\right)\right] + \frac{1}{\hbar^2} g^{h}_{\mathbf{q}} g^{e*}_{\mathbf{q}} p^{*}_{\mathbf{k}} p_{\mathbf{k}+\mathbf{q}} \,, \tag{B1a}$$

$$\frac{d}{dt} t^{(+)}_{-\mathbf{k}-\mathbf{q},\mathbf{k}} = \left(-i\Omega^{(+)}_{-\mathbf{k}-\mathbf{q},\mathbf{k}} - \Gamma^{h}_{-\mathbf{k}-\mathbf{q}} - \Gamma^{e}_{\mathbf{k}}\right) t^{(+)}_{-\mathbf{k}-\mathbf{q},\mathbf{k}} + \left(i\tilde{\mu}_{\mathbf{k}+\mathbf{q}} + \gamma^{e}_{\mathbf{k}+\mathbf{q}}\right) s^{e}_{\mathbf{k}+\mathbf{q},\mathbf{k}} - \left(i\tilde{\mu}_{\mathbf{k}} + \gamma^{h}_{-\mathbf{k}}\right) s^{h}_{-\mathbf{k},-\mathbf{k}-\mathbf{q}}$$
$$- \frac{1}{\hbar^2}\left|g^{e}_{\mathbf{q}}\right|^{2}\left[n_{\mathbf{q}} f^{h}_{-\mathbf{k}-\mathbf{q}} + \left(n_{\mathbf{q}}+1\right)\left(1 - f^{h}_{-\mathbf{k}-\mathbf{q}}\right)\right] p_{\mathbf{k}} - \frac{1}{\hbar^2} g^{e}_{\mathbf{q}} g^{h*}_{\mathbf{q}}\left[n_{\mathbf{q}} f^{e}_{\mathbf{k}} + \left(n_{\mathbf{q}}+1\right)\left(1 - f^{e}_{\mathbf{k}}\right)\right] p_{\mathbf{k}+\mathbf{q}} \,, \tag{B1b}$$

$$\frac{d}{dt} t^{(-)}_{-\mathbf{k},\mathbf{k}+\mathbf{q}} = \left(-i\Omega^{(-)}_{-\mathbf{k},\mathbf{k}+\mathbf{q}} - \Gamma^{h}_{-\mathbf{k}} - \Gamma^{e}_{\mathbf{k}+\mathbf{q}}\right) t^{(-)}_{-\mathbf{k},\mathbf{k}+\mathbf{q}} + \left(i\tilde{\mu}_{\mathbf{k}} + \gamma^{e}_{\mathbf{k}}\right)^{*} s^{e}_{\mathbf{k}+\mathbf{q},\mathbf{k}} - \left(i\tilde{\mu}_{\mathbf{k}+\mathbf{q}} + \gamma^{h}_{-\mathbf{k}-\mathbf{q}}\right)^{*} s^{h}_{-\mathbf{k},-\mathbf{k}-\mathbf{q}}$$
$$- \frac{1}{\hbar^2}\left|g^{e}_{\mathbf{q}}\right|^{2}\left[\left(n_{\mathbf{q}}+1\right) f^{e}_{\mathbf{k}+\mathbf{q}} + n_{\mathbf{q}}\left(1 - f^{e}_{\mathbf{k}+\mathbf{q}}\right)\right] p^{*}_{\mathbf{k}} - \frac{1}{\hbar^2} g^{e}_{\mathbf{q}} g^{h*}_{\mathbf{q}}\left[\left(n_{\mathbf{q}}+1\right) f^{h}_{-\mathbf{k}} + n_{\mathbf{q}}\left(1 - f^{h}_{-\mathbf{k}}\right)\right] p^{*}_{\mathbf{k}+\mathbf{q}} \,, \tag{B1c}$$

with the frequency $\Omega^{(\pm)}_{-\mathbf{k}-\mathbf{q},\mathbf{k}} = \epsilon^{h}_{-\mathbf{k}-\mathbf{q}} + \epsilon^{e}_{\mathbf{k}} \pm \hbar\omega_{op}$ and the relaxation rate $\Gamma^{h}_{\mathbf{k}}$ according to Eqs. (11) and (13) by substituting all electron variables by hole variables.

[1] N. C. Kluksdahl, A. M. Kriman, and D. K. Ferry, Phys. Rev. B **39**, 7720 (1989).
[2] B. L. Al'tshuler, A. G. Aronov, and B. Z. Spivak, Pis'ma Zh. Eksp. Teor. Fiz. **33**, 101 (1981) [JETP Lett. **33**, 94 (1981)].
[3] G. Bergmann, Phys. Rep. **107**, 1 (1984).
[4] S. Schmitt-Rink and D. S. Chemla, Phys. Rev. Lett. **57**, 2752 (1986).
[5] S. Schmitt-Rink, D. S. Chemla, and H. Haug, Phys. Rev. B **37**, 941 (1988).
[6] A. Stahl, Z. Phys. B **72**, 371 (1988).
[7] M. Lindberg and S. W. Koch, Phys. Rev. B **38**, 3342 (1988).
[8] H. Haug, in *Optical Nonlinearities and Instabilities in Semiconductors*, edited by H. Haug (Academic, San Diego, 1988), p. 53.
[9] W. Schäfer, in *Optical Nonlinearities and Instabilities in Semiconductors*, edited by H. Haug (Academic, San Diego, 1988), p. 133.
[10] I. Balslev, R. Zimmermann, and A. Stahl, Phys. Rev. B **40**, 4095 (1989).
[11] A. V. Kuznetsov, Phys. Rev. B **44**, 8721 (1991).
[12] T. Kuhn and F. Rossi, Phys. Rev. Lett. **69**, 977 (1992).
[13] T. Kuhn and F. Rossi, Phys. Rev. B **46**, 7496 (1992).
[14] M. Lindberg, R. Binder, and S. W. Koch, Phys. Rev. A **45**, 1865 (1992).
[15] J. R. Barker and D. K. Ferry, Phys. Rev. Lett. **42**, 1779 (1979).
[16] J. R. Barker and D. K. Ferry, Solid State Electron. **23**, 519 (1980).
[17] J. R. Barker and D. K. Ferry, Solid State Electron. **23**, 531 (1980).

[18] J. Lin and L. C. Chiu, Appl. Phys. Lett. **49**, 1802 (1986).
[19] L. Reggiani, P. Lugli, and A. P. Jauho, Phys. Rev. B **36**, 6602 (1987).
[20] R. Brunetti, C. Jacoboni, and F. Rossi, Phys. Rev. B **39**, 10 781 (1989).
[21] J. Rammer, Rev. Mod. Phys. **63**, 781 (1991).
[22] A. P. Jauho, in *Granular Nanoelectronics*, edited by D. K. Ferry, J. R. Barker, and C. Jacoboni (Plenum, New York, 1991), p. 133.
[23] R. Bertoncini and A. P. Jauho, Phys. Rev. Lett. **68**, 2826 (1992).
[24] F. Rossi and C. Jacoboni, Semicond. Sci. Technol. **7**, B383 (1992).
[25] R. Zimmermann, Phys. Status Solidi B **159**, 317 (1990).
[26] R. Zimmermann, J. Lumin. **53**, 187 (1992).
[27] M. Hartmann and W. Schäfer, Phys. Status Solidi B **173**, 165 (1992).
[28] H. Haug, Phys. Status Solidi B **173**, 139 (1992).
[29] L. Bànyai, D. B. Tran Thoai, C. Remling, and H. Haug, Phys. Status Solidi B **173**, 149 (1992).
[30] F. Rossi, T. Kuhn, J. Schilp, and E. Schöll, in *Proceedings of the 21st International Conference on the Physics of Semiconductors, Beijing, China*, edited by P. Jiang and H. Zheng (World Scientific, Singapore, 1992), p. 165.
[31] D. B. Tran Thoai and H. Haug, Phys. Rev. B **47**, 3574 (1993).
[32] R. Zimmermann and J. Wauer, J. Lumin. **58**, 271 (1994).
[33] J. Schilp, T. Kuhn, and G. Mahler, Semicond. Sci. Technol. **9**, 439 (1994).
[34] H. Haug and C. Ell, Phys. Rev. B **46**, 2126 (1992).
[35] P. Lipavský, V. Špička, and B. Velický, Phys. Rev. B **34**, 6933 (1986).
[36] P. Lipavský, F. S. Khan, A. Kalvová, and J. W. Wilkins, Phys. Rev. B **43**, 6650 (1991).
[37] G. C. Cho, W. Kütt, and H. Kurz, Phys. Rev. Lett. **65**, 764 (1990).
[38] W. Kütt, Adv. Solid State Phys. **32**, 113 (1992).
[39] M. A. Osman and D. K. Ferry, Phys. Rev. B **36**, 6018 (1987).
[40] H. Haug and S. W. Koch, *Quantum Theory of the Optical and Electronic Properties of Semiconductors* (World Scientific, Singapore, 1993).